Electrical conductivity and permittivity measurements near the percolation transition in a microemulsion: I. Experiment

M. T. Clarkson*
Physics Department, Victoria University of Wellington, Wellington, New Zealand

S. I. Smedley
Chemistry Department, Victoria University of Wellington, Wellington, New Zealand
(Received 6 May 1987)

We have made conductivity and permittivity measurements from 5–13 MHz on the microemulsion system toluene–brine–sodium-dodecyl-sulfate–butanol in the region where, by varying the brine salinity, the volume fraction of brine in the microemulsion varies from 0.1 to 0.9 as the system passes from one two-phase region to another via a three-phase region. In the two-phase region at high salinities, where the microemulsion consists of brine droplets dispersed in oil, a percolation transition, identified by a steep rise in the electrical conductivity, and a peak in the permittivity, is observed at brine volume fraction $f_p = 0.130 \pm 0.001$. This transition, although very close to the boundary between the two-phase and three-phase regions, clearly lies inside the two-phase region. The data also suggest that there is a discontinuity in the conductivity at the phase boundary, and we argue that the microemulsion undergoes a change in structure at the phase boundary.

I. INTRODUCTION

Oil-brine-surfactant mixtures with an alcohol added as cosurfactant show an interesting phase behavior. These systems can show[1,2] at low surfactant concentration a three-phase equilibrium, consisting of a microemulsion in contact with an essentially pure oil phase above and a brine phase below. This so-called "middle-phase" microemulsion, which contains similar amounts of cosolubilized oil and brine, consists of continuous paths of both these components, these paths being separated by an interfacial film of surfactant molecules. Scriven[3] was the first to propose such "bicontinuous" structures. Small-angle x-ray scattering experiments[4,5] have given evidence in support of the existence of these structures, and our molecular diffusion measurements[6] have confirmed this structure by showing that the connectivity of oil and water persists over macroscopic distances. It is thought[7] that the alcohol is adsorbed between the hydrocarbon tails of the interfacial surfactant, making the interface more fluid. De Gennes and Taupin[7] have proposed that these structures must have a transient and dynamic nature, in order to explain the low viscosity of the microemulsion.

The three-phase region is of considerable interest because of the very low surface tensions attained at both the microemulsion-oil and microemulsion-brine interfaces.[1,8] If the brine salinity S is decreased from within the three-phase region, both the surface tension of the microemulsion-brine interface and the volume of the brine phase tend continuously towards zero as a "critical" salinity S_1 is approached.[1,8] Below S_1 two phases are observed, a microemulsion consisting of oil droplets dispersed in brine (oil - in - water microemulsion) in contact with an oil phase above. Correspondingly, another critical salinity S_2 is observed at higher salinities. As S_2 is approached from within the three-phase region, both the surface tension and the volume of the oil phase tend continuously towards zero. Above S_2 the microemulsion, which now consists of brine droplets in oil (water-in-oil microemulsion), is in equilibrium with a brine phase below. The structure of the interfaces between the coexisting phases has been elucidated by Beaglehole *et al.*[9] and Meunier.[10]

The nature of the transitions at S_1 and S_2 is not fully understood. In addition to the surface tension behavior, Cazabat *et al.* have observed divergences in the bulk correlation length,[8,11] and peaks in the turbidity[1,8] of the microemulsion at both S_1 and S_2. These phenomena are characteristic of a second-order phase transition. The continuous decrease towards zero of the volumes of the brine and oil phases as S_1 and S_2, respectively, are approached are characteristic of first-order phase transitions. This suggests that S_1 and S_2 are not critical points, but are very near (in the phase diagram) to critical points. However, the ultrasonic absorption coefficients measured by Zana *et al.*[12] are not consistent with this being near-critical behavior. According to Widom[13] S_1 and S_2 are "critical points for second-order phase transitions," as defined by Landau and Lifshitz.[14]

In the toluene–brine–sodium-dodecyl-sulfate–butanol system, our earlier measurements[15] and the measurements of Cazabat *et al.*[16] show a steep rise in the electrical conductivity of the microemulsion in the vicinity of S_2, characteristic of a percolation transition. The steep rise in the conductivity is due to the formation of continuous paths of high-conductivity brine through the sample (which mainly consists of low-conductivity oil), the percolation transition itself being the brine volume fraction at which the first continuous path is formed. It was not clear whether this transition coincides with S_2 or occurs slightly above S_2 in the two-phase region. In the

system studied by Kaler *et al.*[4] it is also not clear whether the percolation transition coincides with S_2 or is in the two-phase region. However, in some systems studied by Salager *et al.*[17] the percolation transition appears to be in the three-phase region.

Here we present the results of a careful study of the conductivity and permittivity in the region near S_2. We have measured the low-frequency (dc) conductivity and permittivity and also the frequency dependence of the conductivity and permittivity over the range 5–13 MHz, for the toluene–brine–sodium-dodecyl-sulfate–butanol system. We have clear evidence that in this system the percolation transition does not coincide with S_2 but occurs inside the two-phase region above S_2. Results also indicate a possible discontinuity in the conductivity at S_2. We argue here that this indicates that the microemulsion undergoes a change in structure at S_2, which is consistent with molecular diffusion measurements.[6]

Our molecular diffusion measurements have also shown the importance of dynamic effects, that is, rapid coalescences, breakups, and fluctuations in shape of microemulsion droplets near S_1 and S_2. In paper II (Ref. 18) our conductivity and permittivity measurements, in particular the frequency dependence, are compared with theories for percolation in static systems and dynamic microemulsion systems to determine what, if any, of the features of our measurements can be attributed to dynamic effects.

II. EXPERIMENTAL

A. Preparation

Pure chemicals were mixed in the following proportions (percentage by weight indicated): toluene, 47.25%; brine (water + NaCl), 46.80%; sodium-dodecyl-sulfate, 1.99%; and butanol, 3.96%. The brine salinity [salinity being the weight NaCl in 100 g of (NaCl + water)] was varied from 1 to 12. The components for the stock solutions were added to 40-cm^3 test tubes with teflon-sealed screw-cap lids, mixed thoroughly, and left for at least two weeks to reach equilibrium in a temperature-controlled air bath at a temperature of 25±2 °C. Two sets of experiments were carried out, a different batch of solutions being prepared for each. For the first we observed $S_1=5.45$ and $S_2=7.55$, while for the second, $S_2=7.25$. We have observed that the positions of the phase boundaries are insensitive to temperature and mixing technique. Meunier[10] has also observed a shift in the phase boundaries for different batches of solutions prepared at the same temperature. It therefore appears unlikely that the shift in the phase boundaries is due to possible systematic errors in the amounts of the components added to the mixture.

B. Impedance measurements

1. Conductance cells

Two cells with cell constants k differing by a factor of 10^3 were constructed to allow accurate measurements to be taken over a conductivity range of six orders of magnitude. Both cells were made of glass with platinum electrodes, and could hold up to 7 ml of liquid. For the low-conductivity water-in-oil microemulsions and the oil phases, a low resistance cell was used, consisting of two parallel-plate electrodes separated by a distance of 2 mm. For the high-conductivity brine solutions and oil-in-water microemulsions, a high resistance cell was used, consisting of two electrodes separated by a glass capillary. The cells were designed so that sample resistance were in general high enough so that effects due to electrode capacitance were negligible.

2. ac measurements

The frequency-dependent conductivity $\sigma(\omega)$ and relative permittivity $\epsilon(\omega)$ (ω denotes angular frequency) of the sample were measured using an HP 4192A LF impedance analyzer, over the frequency range 5–13 MHz. This instrument measures the complex admittance $Y(\omega)=G(\omega)+iB(\omega)$ of the liquid-filled cell, where $i^2=-1$, the conductance $G(\omega)=\sigma(\omega)/k$, and the susceptance $B(\omega)=\epsilon(\omega)\epsilon_0/k$, ϵ_0 being the permittivity of free space.

3. dc conductivity

The dc conductivities were determined in the following manner. The liquid-filled cell was connected in series with a resistor of similar resistance, and the pair connected to a variable dc supply. The voltage-current (V-I) characteristic of the liquid-filled cell was determined from measurements of the supply voltage and the voltage across the resistor. For supply voltages greater than 10 V, the V-I characteristic was usually linear, and the dc conductivity was deduced from the slope.

C. Measurement technique

For each stock solution, measurements were made on all the equilibrium phases present. The conductance cell was carefully filled with the phase to be measured from the stock solution, and a little of the other phase(s). It is not clear whether the microemulsion is a true thermodynamic phase which may be removed from the other equilibrium phases without its properties changing. Rosen and Li[19] have measured a surfactant and cosurfactant density gradient in a "middle-phase" microemulsion in equilibrium with its excess pure phases. This gradient was observed to disappear after the oil phase was removed; the process was reversible, and had a time constant of about 40 days, much longer than the duration of the measurements reported here. In the present experiment, measurements on a microemulsion were always made with the microemulsion in contact with its associated pure phase (or phases). The presence of the oil phase above the microemulsion reduced evaporation of microemulsion components. The filled cell was sealed with a teflon-lined screw cap to reduce evaporation, and placed in the air bath. For the microemulsion and brine phases, a stable reading was usually obtained after 2 h, the time required for thermal equilibrium to be reached. The oil phase required at least 5 h for a stable reading to be obtained, the conductance decreasing during this time.

The first experiments encompassed the entire salinity range, and the results have been reported earlier.[15] The second and more accurate experiments concentrated on the region near the percolation transition. The temperature of the experiment was 25±1 °C.

D. Volume fraction determinations

In a study of percolation it is necessary to know the volume fraction of the percolating component, which in our case is the dispersed brine. For the first experiments, brine volume fractions determined by Pouchelon[20] were used (see Table I). For the more accurate second experiments the volume fractions of the stock solutions used were determined in the following way. We assume that all the water in the microemulsion is in the dispersed brine, and that the composition of the dispersed brine is the same as that of the pure brine phase which is in equilibrium with the microemulsion. The volume fraction f of brine is then given by

$$f=(1+x)\frac{\rho_m}{\rho_b}x_w \ , \tag{1}$$

where x_w is the mass fraction of water in the microemulsion, and ρ_m, ρ_b are the densities of the microemulsion and brine phases, respectively. The quantity x is the mass fraction in the brine phase of the components other than water and has been determined from the measurements of Pouchelon.[20] The densities were determined using 10-ml specific gravity bottles, and x_w was determined directly by a Fisher titration of the microemulsion.

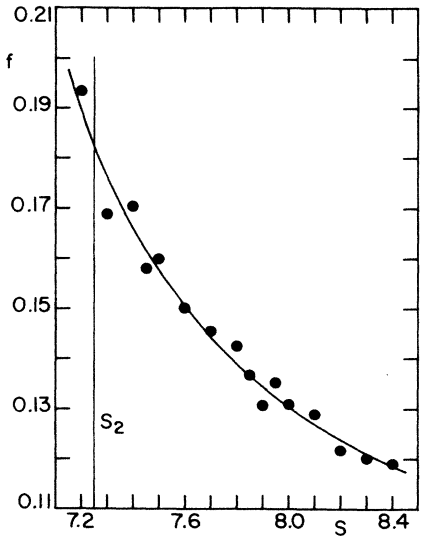

FIG. 1. Brine volume fraction vs brine salinity near the phase boundary at salinity S_2 (vertical line). The curve is a least-squares fit to the data.

III. RESULTS

A. Volume fraction of brine

Volume fraction data for the second experiments are plotted in Fig. 1. There is considerable scatter in the data, probably because these measurements were made

TABLE I. Conductivity data from first run. Conductivities are in s m^{-1}.

S	f	Microemulsion	Brine phase	Oil phase
1.0	0.858	1.912		1.08×10^{-6}
2.0	0.844	3.012		2.06×10^{-6}
3.3	0.826	4.241		2.73×10^{-6}
				3.19×10^{-6}
4.3	0.806	4.90		3.48×10^{-6}
4.6	0.789	5.119		3.46×10^{-6}
5.1	0.763	5.192		4.35×10^{-6}
5.7	0.668	4.272	8.34	1.31×10^{-6}
6.0	0.559	3.355	8.59	3.29×10^{-6}
6.4	0.473	2.598	9.17	6.40×10^{-6}
6.8	0.398	1.624	9.62	4.23×10^{-6}
7.1	0.343	1.23	10.09	2.28×10^{-6}
7.4	0.236	0.628	10.40	3.86×10^{-6}
7.5	0.185	0.377	10.65	
7.6	0.162	0.119	10.73	
7.8	0.149	0.0951	10.74	
7.9	0.145	0.0651	10.97	
8.0	0.143	0.0500	11.27	
8.1	0.140	0.0168	11.36	
8.2	0.138	0.0203	11.26	
8.5	0.131	2.89×10^{-4}	11.88	
8.7	0.125	8.843×10^{-5}	12.08	
9.0	0.118	3.53×10^{-5}	12.34	
9.5	0.105	1.94×10^{-5}	12.94	
10.5	0.080	1.85×10^{-5}	14.16	
12.0	0.042	1.91×10^{-5}	15.55	

TABLE II. Brine volume fraction, conductivity, relative permittivity, relaxation time, and Cole-Cole parameter (second run). Conductivities are in s m^{-1}.

S	f	ϵ	σ	σ_b	T_0 (ns)	α
7.2	0.1898		0.241	10.27		
7.3	0.1767		0.136	10.42		
7.4	0.1662		0.115	10.51		
7.45	0.1617		0.0916	10.51		
7.5	0.1576	10.4	0.0175	10.67		
7.6	0.1504	15.75	0.05036	10.75		
7.7	0.1444	21.5	0.0313	10.84		
7.8	0.1392	29.0	0.0168	11.05	51	0.10
7.85	0.1368	33.0	0.01243	11.04	69	0.13
7.9	0.1347	39.5	6.69×10^{-3}	11.09	167	0.211
7.95	0.1326	42.8	4.46×10^{-3}	11.20	250	0.200
8.0	0.1307	44.0	2.50×10^{-3}	11.22	400	0.203
8.1	0.1272	31.1	4.55×10^{-4}	11.36	267	0.322
8.2	0.1241	21.7	1.82×10^{-4}	11.42	78	0.30
8.3	0.1214	14.8	7.85×10^{-5}	11.54	27	0.23
8.4	0.1189	12.3	6.24×10^{-5}	11.61		

on the solutions after they had been used for the conductivity measurements. It is therefore necessary to fit a curve to the data, and the most appropriate curve can be found from theoretical considerations. We assume that the microemulsion consists of only two components, oil and brine. Let V_b and V_t be the volumes of brine and oil in the initial mixture (total volume $V_T = V_b + V_t$), and let V_m be the volume of microemulsion. It can be shown from purely volumetric constraints that

$$\frac{V_m}{V_T} = \frac{1}{(1-f)(1+V_b/V_t)} . \tag{2}$$

If we assume that the area of interface per surfactant molecule is constant and that all the surfactant is in the microemulsion, then A_T, the total area of interface in the microemulsion, is constant. If the microemulsion consists of spherical droplets of radius R, then

$$f = \frac{A_T R}{3V_m} . \tag{3}$$

Combining Eqs. (2) and (3) gives

$$R = \frac{1}{\beta}\frac{f}{1-f} , \tag{4}$$

where $\beta = A_T(1+V_b/V_t)/3V_T$ is a constant. The ions present in the brine screen the electrostatic repulsion between the anionic heads of the surfactant molecules, consequently the curvature of the interface, and therefore R, is a function of brine salinity. A simple model in which spheres expand to $R=\infty$ at S_0 gives

$$R \propto \frac{1}{1-(S_0/S)^n} , \quad S > S_0 \tag{5}$$

where S_0, the salinity at which the interface has no preferential curvature, is near the middle of the three-phase region. Hwan, Miller, and Fort[21] suggest that $n=\frac{1}{2}$. Combining Eqs. (4) and (5) gives

$$\frac{f}{1-f} \propto \frac{1}{1-(S_0/S)^n} , \quad S > S_0 . \tag{6}$$

A least-squares fit of this curve was made to our data. An acceptable fit could be obtained only if a constant term was added to the right-hand side of Eq. (6). the quality of fit was sensitive to the choice of S_0, but insensitive to n. For the fitted curve in Fig. 1, $S_0=6.5$ and $n=1$, and the constant term was 3.70. Values of f from the least-squares fit are tabulated in Table II.

B. Low-frequency conductivity and permittivity

The frequency dependence of the conductivity $\sigma(\omega)$ and relative permittivity $\epsilon(\omega)$ of the microemulsion for selected samples from the second batch are shown in Figs. 2(a) and 2(b), respectively. These show plateaus in both $\sigma(\omega)$ and $\epsilon(\omega)$ at low frequencies ($\sim$100 kHz). At lower frequencies, the electrode capacitance causes $\epsilon(\omega)$ to increase [Fig. 2(b)]. At higher frequencies, generally greater than 1 MHz, $\sigma(\omega)$ increases and $\epsilon(\omega)$ decreases with increasing frequency due to a relaxation of the polarization of the oil water interfaces in the microemulsion (the Maxwell-Wagner effect): The analysis in Paper II will confirm this interpretation. The plateaus in $\sigma(\omega)$ and $\epsilon(\omega)$ correspond to the low-frequency (dc) conductivity σ and relative permittivity ϵ, respectively, of the microemulsion. Similar plateaus were observed for the oil and brine phases, although plateaus in the permittivity of the brine phase could not be observed due to resonances resulting from the inductance in the leads.

Values of the low-frequency conductivities for the first experiments have been plotted versus brine salinity and brine volume fraction in Fig. 3 and are tabulated in Table I. Values of the low-frequency relative conductivity σ_r and relative permittivity ϵ of the microemulsion for the second experiments have been plotted versus brine volume fraction in Figs. 4(a) and 4(b) and are tabulated in

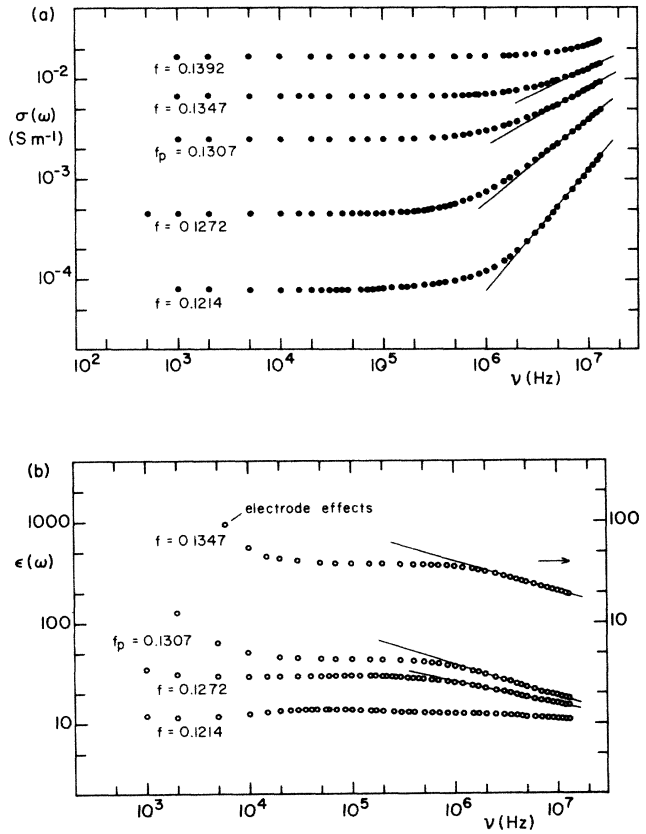

FIG. 2. (a) Conductivity $\sigma(\omega)$ and (b) relative permittivity $\epsilon(\omega)$ vs frequency (data from second experiments).

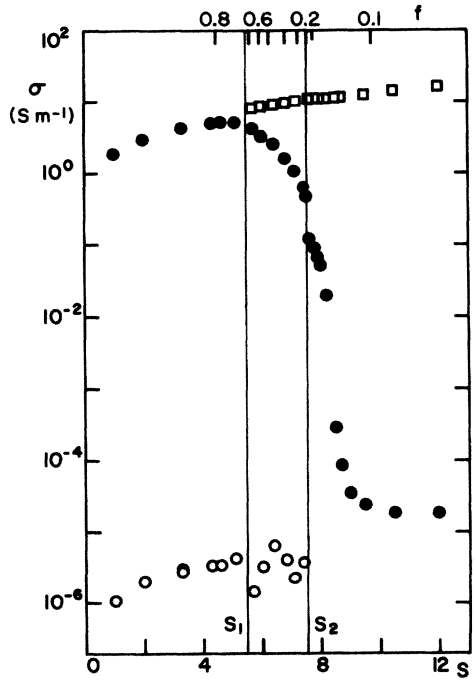

FIG. 3. Low-frequency conductivity vs brine salinity and brine volume fraction (data from first experiments). Closed circles, microemulsion; open circles, oil phase; open squares, brine phase. The vertical lines are the phase boundaries (salinities S_1 and S_2).

Table II. The relative conductivity $\sigma_r=\sigma/\sigma_b$ has been calculated to allow for the variation of the brine conductivity σ_b with salinity.

1. *Microemulsion phase*

In Fig. 3 we see that the conductivity σ of the microemulsion rises by six orders of magnitude from a conductivity comparable to that of the oil phase at high salinity (low brine content) to a conductivity comparable to that of the brine phase at low salinity (high brine content). In the two-phase region at low salinities ($S<S_1$) the conductivity of the microemulsion is mainly determined by the salinity of the brine. For $S>S_2$ the fraction of brine mainly determines the conductivity of the microemulsion. We expect that these low-frequency conductivity values will be equal to the measured dc conductivity values, and indeed, for $S<S_2$, the two values agree to within 5%. The agreement was poorer ($\sim 10\%$) at higher salinities ($S\simeq 10$), probably because of the uncertainties in the high resistances involved. At intermediate salinities, sample resistances were unsuitable for dc measurements. Pouchelon[20] has also made conductivity measurements on a system of the same composition as the system studied here, some of which are presented in Ref. 16. Our data show good agreement with the data of Pouchelon, except at high salinities ($S>8.0$) where our conductivity values are much lower.

Our low-frequency conductivity and permittivity data from the second experiments, plotted versus brine volume fraction [Figs. 4(a) and 4(b)], clearly show that the permittivity ϵ reaches a peak at the brine volume fraction where the gradient of the $\log_{10}\sigma_r$ curve is a maximum. We conclude that this volume fraction corresponds to the percolation transition, occurring at $f_p=0.130\pm0.001$. Efros and Shklovskii[22] have predicted that a finite peak in the permittivity occurs at the percolation transition if the insulating component has a nonzero conductivity. Preliminary relative permittivity values from the first run were presented earlier,[15] but an error near f_p has been noted. We analyzed there the data in terms of R-C networks, noting that the behavior at low frequencies can be approximated by a parallel R-C network of capacitance C and resistance R which is in series with a resistance R_s. We proceeded to estimate ϵ from the capacitance C, $\epsilon=kC/\epsilon_0$. However, we neglected to realize that this is valid only if $R\gg R_s$, which is not true near f_p. The corrected values indicate a peak at f_p, in confirmation of the second set of more accurate data presented here.

2. *Brine phase*

The conductivity of the brine phase shows good agreement (within 1%) with the data for pure brine taken from the literature.[23] (The brine phase contains about 2% by weight of surfactants.[20]) As mentioned earlier, the observed S_2 for the second batch was lower by an amount $\Delta S=0.4$ than observed for the first batch. It is possible that this apparent shift in salinity was due to a systematic error in the amount of NaCl added to the mixtures in each batch. However, in this case we would expect the

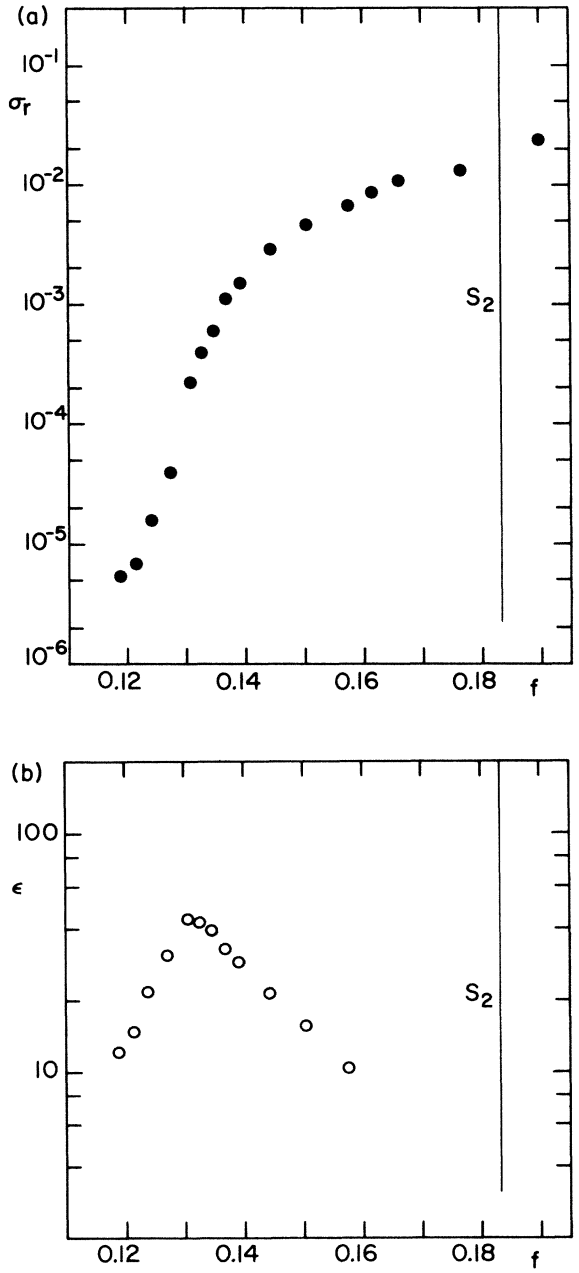

FIG. 4. (a) Low-frequency relative conductivity σ_r and (b) relative permittivity ϵ vs brine volume fraction (data from second experiments) near the phase boundary S_2 (vertical line).

conductivities of the brine phases from the two batches to differ by about 4%, and this difference is not apparent in our data.

3. *Oil phase*

The behavior of the measured oil phase conductivity shows a remarkable dependence on the phase behavior of the system (Fig. 3). There appears to be a discontinuity in the conductivity at S_1. In the three-phase region, starting at S_1, the conductivity rises to a maximum at $S=6.4$ near the middle of this region, then falls to a minimum at $S=7.1$ before apparently rising again as the oil phase becomes turbid near S_2.

The magnitude of the oil phase conductivity is much higher than the value of $\sigma=10^{-12}-10^{-10}$ s m^{-1} for pure toluene,[24] and this is presumably due to the presence of surfactant and NaCl ions. The concentration of ions is low. van Nieuwkoop and Snoei[25] have analyzed the composition of the oil phase in the three-phase region of a system identical to the system studied here except that the oil is heptane rather than toluene. They have measured a sodium dodecyl sulfate concentration $\sim 0.02\%$ and could not detect the presence of chloride ions. Given a low concentration of surfactant ions, it is not inconceivable that, considering the long time needed for the oil phase conductivity to reach a steady value, the conductivity may be dominated by the adsorption of surfactant on to the electrodes. However, we have observed that the oil phase is very sensitive to thermal or mechanical disturbance. Once disturbed, the phase becomes cloudy and it then takes several hours for the phase to settle down again. The observed low-frequency relative permittivity of the oil phase was essentially independent of frequency and was measured to be $\epsilon=2.9$.

C. High-frequency data

In an inhomogeneous medium interfacial polarization[26] causes a dispersion in the permittivity accompanied by a peak in the dielectric loss $\Delta\epsilon''(\omega)=[\sigma(\omega)-\sigma]/\omega\epsilon_0$, where σ is the low-frequency conductivity, at a characteristic frequency ω_0 (the Maxwell-Wagner effect). In our samples near f_p, ω_0 was sufficiently low for part of this relaxation behavior to be observed. The relaxation is usually characterized by a Cole-Cole plot (after Cole and Cole[27]), in which $\Delta\epsilon''(\omega)$ is plotted against $\epsilon(\omega)$. Cole-Cole plots for our data are shown in Figs. 5(a) and 5(b).

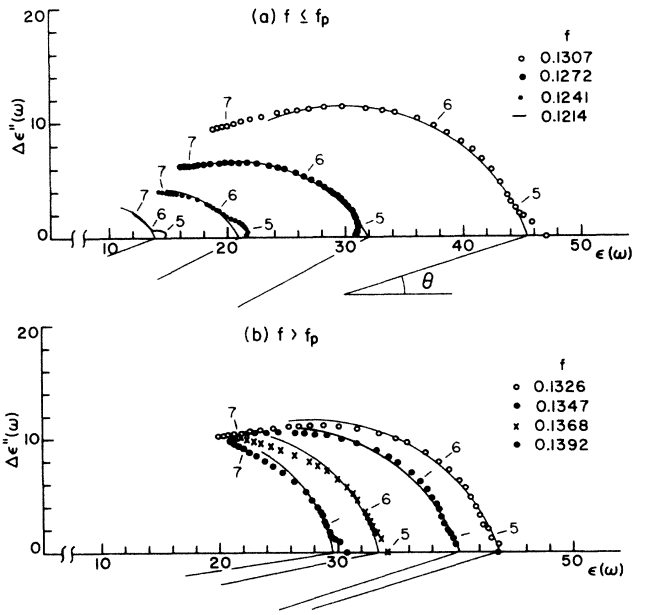

FIG. 5. Cole-Cole plots for the data from the second experiment (a) $f \leq f_p$, (b) $f > f_p$. The numbers 5, 6, and 7 are $\log_{10}\nu$, where ν is the frequency in Hz.

D. Minor relaxation

In the Cole-Cole plots for samples of salinity 8.2 or greater (volume fraction 0.1241 or less), there appears in addition to the main relaxation also a smaller relaxation at lower frequencies ($\sim$100 kHz). This feature, shown more clearly in Fig. 6, could possibly arise from systematic extraneous experimental errors such as electrode effects, effects of the cell geometry or construction, or effects due to the impedance analyzer. However, the following tests give strong evidence that this minor relaxation is a property of the microemulsion. Electrode effects are observed at much lower frequencies (Fig. 2), so these are not a possibility. A cell having a different geometry was used to test whether the apparent relaxation is due to the geometry and/or construction of the parallel-plate cell. This cell consisted of two platinum-black wire electrodes enclosed in a glass bulb. Measurements on a new sample were made consecutively with this cell and with the parallel-plate cell, and these measurements with each cell show evidence for this relaxation, but the relative sizes of the apparent relaxations are different. However, the height of the dielectric loss peak of the apparent relaxation is sensitive to the value of σ chosen to calculate the dielectric loss. Therefore, the effect does not appear to be due to the cell geometry or cell construction. To test whether this effect is due to the instrument, an R-C network was constructed to simulate the main relaxation only. Measurements on this circuit showed no additional effect comparable to that seen in Fig. 6.

This relaxation was apparent for salinities up to $S=9.5$. At higher salinities ($S=10.5$ and $S=12.0$), and in the more highly conducting oil phases, there was also evidence for this relaxation, but it was much smaller and difficult to resolve.

IV. DISCUSSION

A. Percolation transition

Our data clearly show that in this system the percolation transition lies inside the two-phase region at high salinities, and not at the boundary between the two-phase and three-phase systems S_2. Therefore, while S_2 is not a percolation transition, it is very close to, and possibly related to, the percolation transition, as suggested by Cazabat *et al.*[16]

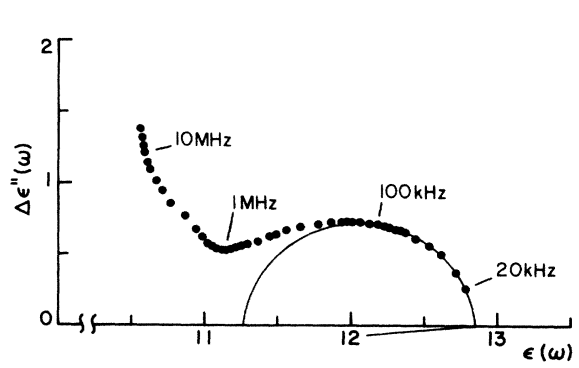

FIG. 6. Cole-Cole plot of minor relaxation for $S=8.4$ (data from second experiments).

van Dijk[28] and Bhattacharya *et al.*[29] have also recently observed peaks in the permittivity in their studies of percolation in other microemulsion systems. The peaks observed by van Dijk reach a height of $\epsilon\sim80$, while the peak observed by Bhattacharya *et al.* reaches $\epsilon\sim30$, both being similar to the height of our peak ($\epsilon\sim40$).

B. Dynamic effects

van Dijk[28] has observed a peak in the permittivity near the conductivity percolation transition in the water-sodium di-2-ethylhexylsulfosuccinate (AOT)-iso-octane microemulsion system. In van Dijk's data, the conductivity transition appears at a lower water fraction than the permittivity peak, although the latter is not well defined. van Dijk suggests that this apparent lowering of the conductivity transition may be due to the microscopic dynamical phenomena evident in these systems. However, in our data [Figs. 4(a) and 4(b)] the permittivity peak coincides exactly with the conductivity transition. Molecular diffusion measurements[6] have shown that in the region of the percolation transition in the system studied here, the dispersed droplets are undergoing rapid coalescences, breakups, and fluctuations in shape. Therefore, in the system studied here, these microscopic dynamical phenomena do not cause a lowering of the position of the conductivity transition relative to the position of the permittivity peak. In paper II the effects of the dynamic nature of the microemulsion are discussed further.

C. Conductivity near S_2

The data reveal a possible discontinuity in the low-frequency conductivity at S_2 (Fig. 7). We have previously reported[6] that there is no apparent discontinuity in the molecular diffusion coefficient at S_2 (and at S_1). The size of the conductivity discontinuity, if it is real, suggests that if a similar discontinuity is present in the diffusion coefficient, then we did not make measurements near enough to S_2 to observe it.

Our molecular diffusion measurements[6] suggest that at S_2 the dispersed brine is contained in random pathways which are locally one dimensional in structure. Therefore, while at the percolation transition the first continuous brine path is formed, at S_2 most of the microemulsion contains continuous paths. We therefore suggest the following tentative explanation of the discontinuity in the conductivity at S_2. As S_2 is approached from within the two-phase region, the brine droplets coalesce into random, locally one-dimensional structures. Below S_2, in the three-phase region, these structures begin to coalesce into the random, locally two-dimensional structure apparent near the middle of the three-phase region.[6] Such a model could explain the apparently different conductivity trends above and below S_2.

D. Frequency dependence

Dielectric relaxation can often be represented by a circular arc in the ϵ-$\Delta\epsilon''(\omega)$ plane, with the center of the circle frequently being depressed below the $\epsilon(\omega)$ axis. In molecular relaxation, this depression of the Cole-Cole

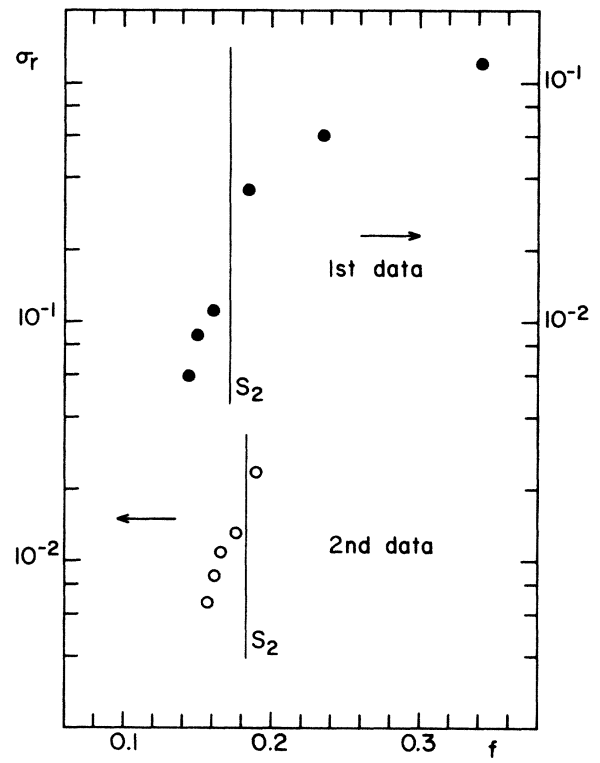

FIG. 7. Conductivity near the phase boundary S_2 vs brine volume fraction.

plot is an indication of a distribution of relaxation times.[30] A measure of the degree of depression is the parameter α, where $\theta=\alpha\pi/2$ is the angle indicated in Fig. 5(a). Dielectric relaxation due to interfacial polarization in a water-in-oil emulsion which does not show a percolation transition or is far from the percolation transition usually has the form of a symmetric semicircle in the $\epsilon(\omega)$-$\Delta\epsilon''(\omega)$ plane,[26] and for small f the high frequency limit ϵ_h of the relative permittivity is approximately

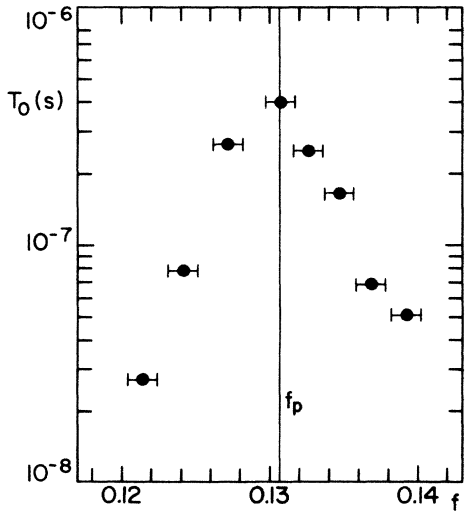

FIG. 8. Characteristic relaxation time T_0 vs brine volume fraction (data from second experiments) near the percolation transition f_p.

equal to the relative permittivity of the oil.

For our samples near f_p, circular arcs give a reasonable approximation to the shape of the Cole-Cole plots [see Figs. 5(a) and 5(b)]. However, extrapolation of these arcs to higher frequencies yield values of ϵ_h which are much higher than the expected value of $\epsilon_h \simeq 2$. This suggests that the experimental Cole-Cole plots near the percolation transition are not completely semicircular, but have an unsymmetrical shape. We have determined values of the parameter α from our data, and these are listed in Table II. We find that α increases as f_p is approached from below, but shows little variation above f_p.

We have also determined a characteristic relaxation time $T_0=2\pi/\omega_0$ for the relaxation evident in samples near f_p. In general, ω_0 was determined by finding the frequency at which $\Delta\epsilon''(\omega)$ reaches a peak. In samples in which the peak in $\Delta\epsilon''(\omega)$ was above the measurement range, ω_0 was estimated in the following way. In the region of the dielectric relaxation, $\log_{10}\sigma(\omega)$ shows a linear variation with $\log_{10}\omega$ [see Fig. 2(a)]. This linear variation was extrapolated until a peak in the dielectric loss was obtained. Values of T_0 are plotted in Fig. 8 and are tabulated in Table II. Clearly T_0 reaches a peak at f_p.

E. Minor relaxation

The apparent small relaxation in the kHz region observed in samples below the percolation transition can be approximated by a semicircle in the $\Delta\epsilon''(\omega)$-$\epsilon(\omega)$ plane (Fig. 6). It is therefore possible to estimate the dielectric increment $\Delta\epsilon=\epsilon-\epsilon_h$ and characteristic frequency $\omega_0/2\pi$ of the relaxation as a function of salinity (or brine volume fraction). The results of this analysis are given in Table III. Schwan *et al.*,[31] Sasaki *et al.*,[32] and Springer *et al.*[33] in their dielectric studies on suspensions of polystyrene latex particles in aqueous brine, have also observed dielectric relaxation in the kHz region. These authors interpret their observed relaxation as being a relaxation of the double layer formed by the ions (counterions) bound to the surface of the colloidal latex particles. Schwarz[34] has developed a theory for the relaxation of a double layer around spherical particles in which the relaxation is of the Debye form with the dielectric increment $\Delta\epsilon$ and characteristic angular frequency ω_0 given by

$$\Delta\epsilon=\tfrac{9}{4}f(1+\tfrac{1}{2}f)^{-2}(q_0^2R\sigma_0/\epsilon_0kT)\ , \tag{7}$$

TABLE III. Characteristics of the minor relaxation.

S	f	$\Delta\epsilon$	$\omega_0/2\pi$ (kHz)
First batch			
8.7		1.3	200
9.0		0.65	150
9.5		0.25	150
Second batch			
8.3	0.1214	1.4	250
8.4	0.1189	1.6	140

$$\omega_0 = \frac{2D_b}{R^2}\ , \tag{8}$$

where f is the volume fraction of spheres, R is the sphere radius, σ_0 is the surface charge density of the counterions bound to the sphere, q_0 is the electronic charge, and D_b is the diffusion coefficient of the counterions.

For a brine droplet in a water-in-oil microemulsion, the negatively charged surfactant chains at the interface can attract ions either from the oil phase outside, or from the brine inside the droplet. Thus, there is the possibility for a double layer on the outside or the inside of the droplet. The Schwarz theory, in which the particles are rigid spheres, cannot be expected to be applicable to a dynamic microemulsion near the percolation transition, but two points are worth noting: (i) the Schwarz theory predicts that $\Delta\epsilon$ increases with f, as was observed, and (ii) we can estimate the value of ω_0 predicted by Eq. (8). Near f_p, $R \sim 40$ nm. To estimate D_b, we assume the mobility of the ions to be the same as that of the surfactant chains at the interface. Roeder *et al.*[35] have measured the diffusion coefficient of surfactant molecules along a lamellar surface to be $D \sim 10^{-9}$ m^2 s^{-1}. Using this as an estimate of D_b, we find $\omega_0/2\pi \sim 10$ kHz, which is comparable to the observed values.

The relaxation of a double layer at the surface of the microemulsion droplets thus does offer a possible explanation for the dielectric relaxation observed in the kHz region for samples below the percolation transition.

ACKNOWLEDGMENTS

M.T.C. wishes to thank Professor D. Beaglehole for his supervision, and the Chemistry Department at Victoria University of Wellington for their hospitality. M.T.C. also acknowledges financial support from the New Zealand Energy Research and Development Committee. The water fraction determinations were carried out at the Applied Chemistry Section of the Chemistry Division of the New Zealand Department of Scientific and Industrial Research.

*Present address: Department of Applied Mathematics, Research School of Physical Sciences, The Australian National University, A.C.T. 2601, Australia.

[1]A. Pouchelon, J. Meunier, D. Langevin, D. Chatenay, and A. M. Cazabat, Chem. Phys. Lett. **76**, 277 (1980).

[2]A. M. Bellocq, J. Biais, B. Clin, A. Gelot, P. Lalanne, and B. Lemanceau, J. Colloid Interface Sci. **74**, 311 (1980).

[3]L. E. Scriven, Nature **263**, 123 (1976).

[4]E. W. Kaler, K. E. Bennett, H. T. Davis, and L. E. Scriven, J. Chem. Phys. **79**, 5673 (1983); E. W. Kaler, H. T. Davis, and L. E. Scriven, *ibid.* **79**, 5685 (1983).

[5]L. Auvray, J.-P. Cotton, R. Ober, and C. Taupin, J. Phys. **45**, 913 (1984).

[6]M. T. Clarkson, D. Beaglehole, and P. T. Callaghan, Phys. Rev. Lett. **54**, 1722 (1985).

[7]P. G. de Gennes and C. Taupin, J. Phys. Chem. **86**, 2294 (1982).

[8]A. M. Cazabat, D. Langevin, J. Meunier, and A. Pouchelon, Adv. Colloid Interface Sci. **16**, 175 (1982).

[9]D. Beaglehole, M. T. Clarkson, and A. Upton, J. Colloid Interface Sci. **101**, 330 (1984).

[10]J. Meunier, J. Phys. Lett. **46**, L1005 (1985).

[11]A. M. Cazabat, D. Langevin, J. Meunier, and A. Pouchelon, J. Phys. Lett. **43**, L89 (1982).

[12]R. Zana, J. Lang, O. Sorba, A. M. Cazabat, and D. Langevin, J. Phys. Lett. **43**, L829 (1982).

[13]B. Widom, J. Chem. Phys. **81**, 1030 (1984).

[14]L. D. Landau and E. M. Lifshitz, *Statistical Physics* (Pergamon, New York, 1958), p. 455.

[15]D. Beaglehole and M. T. Clarkson, in *Localization and Metal-Insulator Transitions,* edited by H. Fritzsche and D. Adler (Plenum, New York, 1985), p. 153.

[16]A. M. Cazabat, D. Chatenay, D. Langevin, and J. Meunier, Faraday Discuss. Chem. Soc. **76**, 291 (1982).

[17]J. L. Salager, M. Miñana-Pérez, M. Pérez-Sánchez, M. Ramírez-Gouveia, and C. J. Rojas, J. Dispersion Sci. Techn. **4**, 313 (1983).

[18]M. T. Clarkson, Phys. Rev. A **37**, 2079 (1988).

[19]M. J. Rosen and Z.-P. Li, J. Colloid Interface Sci. **97**, 456 (1984).

[20]A. Pouchelon, thesis, Université Pierre et Marie Curie, Paris, 1983.

[21]R.-N. Hwan, C. A. Miller, and T. Fort, J. Colloid Interface Sci. **68**, 221 (1979).

[22]A. L. Efros and B. I. Shklovskii, Phys. Status Solidi B **76**, 475 (1976).

[23]*Landolt-Börnstein: Zahlenwerte und Funktionen aus Physik, Chemie, Astronomie, Geophysik und Technik,* edited by K. Hellwege, A. M. Hellwege, K. Shäfer, and E. Lax (Springer-Verlag, Berlin, 1960), Vol. 2, Part. 7, p. 53.

[24]*Landolt-Börnstein: Zahlenwerte und Funktionen aus Physik, Chemie, Astronomie, Geophysik und Technik,* edited by K. H. Hellwege and A. M. Hellwege (Springer-Verlag, Berlin, 1962), Vol. 2, Part. 8, pp. 5–849ff.

[25]J. van Nieuwkoop and G. Snoei, J. Colloid Interface Sci. **103**, 400 (1985).

[26]T. Hanai, in *Emulsion Science,* edited by P. Sherman (Academic, London, 1968), p. 353.

[27]K. S. Cole and R. H. Cole, J. Chem. Phys. **9**, 341 (1941).

[28]M. A. van Dijk, Phys. Rev. Lett. **55**, 1003 (1985).

[29]S. Bhattacharya, J. P. Stokes, M. W. Kim, and J. S. Huang, Phys. Rev. Lett. **55**, 1884 (1985).

[30]J. B. Hasted, *Aqueous Dielectrics* (Chapman and Hall, London, 1973).

[31]H. P. Schwan, G. Schwarz, J. Maczuk, and H. Pauly, J. Phys. Chem. **66**, 2626 (1962).

[32]S. Sasaki, A. Ishikawa, and T. Hanai, Biophys. Chem. **14**, 45 (1981).

[33]M. M. Springer, A. Korteweg, and J. Lyklema, J. Electroanal. Chem. **153**, 55 (1983).

[34]G. Schwarz, J. Phys. Chem. **66**, 2636 (1962).

[35]B. W. Roeder, E. E. Burnell, A. L. Kuo, and C. G. Wade, J. Chem. Phys. **64**, 1848 (1976).